Desalination and Water Treatment
www.deswater.com
doi: 10.5004/dwt.2018.22368

114 (2018) 297–306
May

Modification of activated carbons by HNO_3 and H_2O_2 for removal of methylene blue dye from aqueous solutions

Liheng Liu[a,b,c], Hua Lin[a,b,c,*], Fei Pan[a,b,c], Geng Wang[a,b,c], Dunqiu Wang[a,b,c,*]

[a]*College of Environmental Science and Engineering, Guilin University of Technology, Guilin 541004, China, Tel./Fax: +86 (773) 2536922; emails: linhua5894@163.com (H. Lin), wangdunqiu@sohu.com (D. Wang), deanhenry_liu01@126.com (L. Liu), 361281014@qq.com (F. Pan), deepluvboa@163.com (G. Wang)*
[b]*Guangxi Key Laboratory of Environmental Pollution Control Theory and Technology, Guilin University of Technology, Guilin 541004, China*
[c]*Collaborative Innovation Center for Water Pollution Control and Water Safety in Karst Area, Guilin University of Technology, Guilin 541004, China*

Received 16 September 2017; Accepted 8 April 2018

ABSTRACT

A commercial granular activated carbon (GAC-C) was used as raw adsorbent, and modified by nitric acid and hydrogen peroxide. The modified samples were named as GAC-N (nitric acid) and GAC-H (hydrogen peroxide). The optimum conditions of different modifiers were determined by single factor and orthogonal experiments, while the adsorption amount of methylene blue (MB) was used as the evaluation index. The modification could significantly improve the mesopore volumes of adsorbents, and introduce oxygen-containing functional groups on its surface, which played an important role in MB adsorption process. The optimum conditions for the two modifiers are consistent, that is, modification temperature = 90°C, modifier concentration = 2 mol/L, contact time = 4 h, and adsorbent dose = 0.2 g/mL. The MB adsorption capacities of GAC-C, GAC-N, and GAC-H were 22.44, 28.33, and 25.12 mg/g, respectively. The MB adsorption was a heterogeneous and monolayer process in which chemisorption was dominant. Moreover, the MB adsorption process followed the pseudo-second-order model. The intraparticle diffusion was the rate-controlling step.

Keywords: Oxidation modification; Activated carbons; Process optimization; Methylene blue dye; Adsorption

1. Introduction

With the development of economy and population growth, the demand for dyes in many fields (e.g., textile, paper, leather tanning, plastic, carpet, food, and cosmetics [1]) is rapidly increasing in the last decades, causing a lot of wastewater containing dyes was produced and directly discharged into natural water bodies like rivers and lakes [2]. The direct discharge of dye wastewater could cause great harm to plants, animals, and humans [3,4] because the dyes are generally strongly toxic or there are a lot of suspended solids in the dye wastewater [5,6]. For example, methylene blue (MB) is a cationic dye widely used in cotton, wood, fiber, and silk dyeing [7], which would result in some health risks, such as vomiting, nausea, tissue necrosis, eyes injury, diarrhea, jaundice, quadriplegia, and methemoglobinemia [8–11]. Therefore, it is very necessary to remove the dyes from the wastewater before the discharge.

According to the characteristics of dye wastewater, a series of techniques, such as flocculation, biodegradation, photo catalysis, oxidation, electrolysis, adsorption, and ion exchange [12,13], have been developed to remove the dyes. In the above methods, adsorption is considered to be one of the most well-known and economic techniques for dyes removal because of its high efficiency, easy operation, recyclability [14], and strong removal ability for most dyes by

* Corresponding author.

different adsorbents [7]. Consequently, a large number of adsorbents have been used to evaluate the removal efficiency for dyes by adsorption [15–18]. Among these adsorbents, activated carbon is the most commonly used adsorbent.

In general, the adsorption capability of activated carbon for contaminants depends on the nature of activated carbon [19], in particular its specific surface area, pore structure, and surface functional groups [20,21]. Furthermore, the results of some research showed that surface modification could improve the adsorption effectiveness and selectivity of adsorbents for certain contaminants [22,23]. The surface modification methods include chemical modification, physical modification, microwave treatment, and impregnation [24]. Comparing with the other methods, the chemical modification is the most usually used method, and the common chemical modification agents are mainly nitric acid, hydrogen peroxide, sulfuric acid [25], and other chemical agents with strong oxidizing properties, such as zinc chloride and phosphoric acid [26]. At present, there are many researches on the adsorption and removal of MB by modified activated carbons [22,24,26], while few studies focus on the effects of modifiers on MB removal. The literature search results showed that only Shih [27] specifically discussed the effect of nitric acid, hydrochloric acid, and sulfuric acid on MB adsorption of clean rice husks.

In this study, the effect of nitric acid and hydrogen peroxide on MB adsorption of commercial granular activated carbons (GAC-Cs) was discussed. The optimum modification conditions of different agents were investigated through orthogonal experiments and single factor analysis, while the MB adsorption capacity of adsorbent was considered as an evaluation index. The adsorption mechanism was also discussed through the characterization of the products and analysis of the MB adsorption data.

2. Materials and methods

2.1. Materials

The commercial GAC-Cs were supplied by Tianjin Guangfu Technology Development Co., Ltd., China. MB, nitric acid, and hydrogen peroxide were purchased from Xilong Science Co., Ltd., China, and AR.

2.2. Modification of granular activated carbons

The commercial GAC-C samples were first washed with deionized water several times to remove surface dust and impurities. When the pH of the washed filtered water was neutral, the samples were dried for 12 h at 105°C. And then, the dried samples were placed in a desiccator.

The different doses of pretreated GAC-Cs were added into 150 mL volumetric flasks which were filled with 100 mL modifier with different concentration. Subsequently, the volumetric flasks were put into the constant temperature water bath oscillators. After some time, the samples were washed with deionized water until the pH was stable. Finally, the samples were also dried for 12 h at 105°C. The modified samples under optimum conditions were designated as GAC-N (nitric acid) and GAC-H (hydrogen peroxide), respectively.

2.3. Adsorption of methylene blue

To evaluate the effect of modification on MB adsorption capacity, and discuss its adsorption isotherms and kinetics, a series of experiments were carried out. First, 0.05 g of the adsorbent was added to 50 mL of the MB solution. Then the solution was shaken in a temperature-controlled water bath shaker for 4 h. The concentrations of MB were measured by a UV-vis spectrophotometer (UV-6100A) at 665 nm. The MB adsorption amount at equilibrium and time t, q_e (mg/g) and q_t (mg/g) were calculated by the following two equations [28–30]:

$$q_e = \frac{C_0 - C_e}{W} V \tag{1}$$

$$q_t = \frac{C_0 - C_t}{W} V \tag{2}$$

where C_0, C_t, and C_e (mg/L) are MB concentrations at initialization, time t, and equilibrium, respectively; V (L) and W (g) are solution volume and adsorbent dosage, respectively. The relationship between Eqs. (1) and (2) is as follows:

$$\frac{q_t}{q_e} = \frac{C_0 - C_t}{C_0 - C_e} \tag{3}$$

2.4. Characterization

In order to discuss the effect of modification on surface characteristics, various analytical methods were used to characterize the raw and modified adsorbents. The surface topography and porous structure of all samples were detected using a scanning electron microscope (SEM, JEOL JSM-6380LV) and the N_2 adsorption isotherm at 77 K (Quantachrome Autosorb-1-C). The porous structure parameters were calculated by the methods of reference [30]. Fourier transform infrared spectroscopy (FTIR, Thermo Nicolet 470FT-IR) was used to identify the surface functional groups of all samples before and after adsorption.

3. Results and discussion

3.1. Characterization of adsorbents modified

3.1.1. Porous structure

Fig. 1 shows the nitrogen adsorption/desorption isotherm curves of GAC-C, GAC-N, and GAC-H at 77 K. Based on the IUPAC (International Union of Pure and Applied Chemistry) classification, the curves are type IV adsorption/desorption isotherm, suggesting the mesopores of the samples are dominant. The pore size distributions of the three samples (Fig. 2) also indicate they are all mesoporous adsorbents.

The porous structure parameters calculated by Brunauer–Emmet–Teller (BET) equation, t-plot method, and Barrett–Joyner–Halenda model are listed in Table 1. The modification could improve the surface area and pore volume. The effect of nitric acid is greater than hydrogen peroxide because of its stronger oxidation.

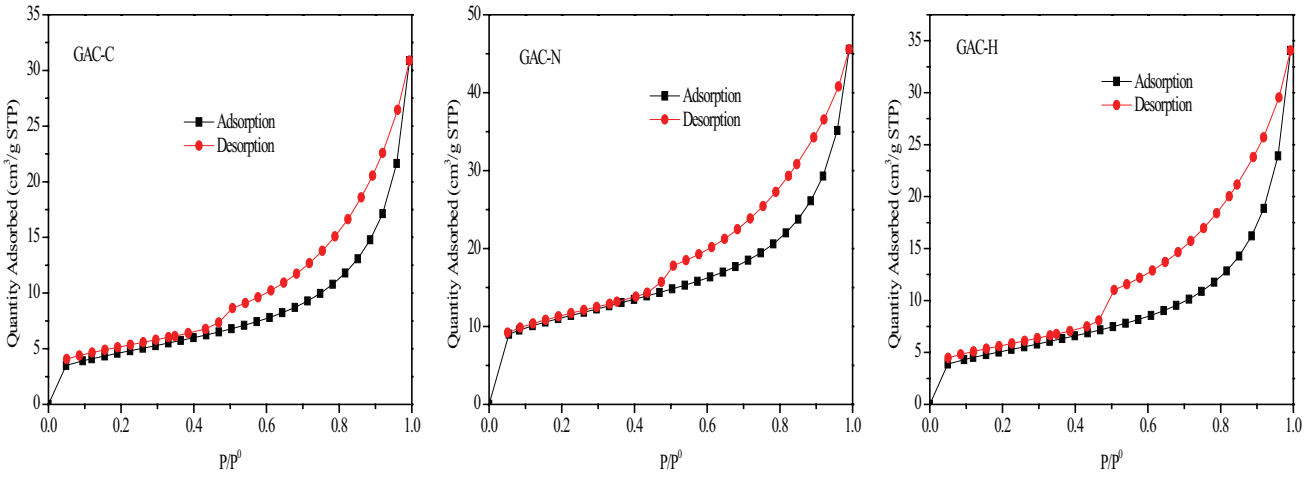

Fig. 1. Nitrogen adsorption/desorption isotherms of GAC-C, GAC-N, and GAC-H at 77 K.

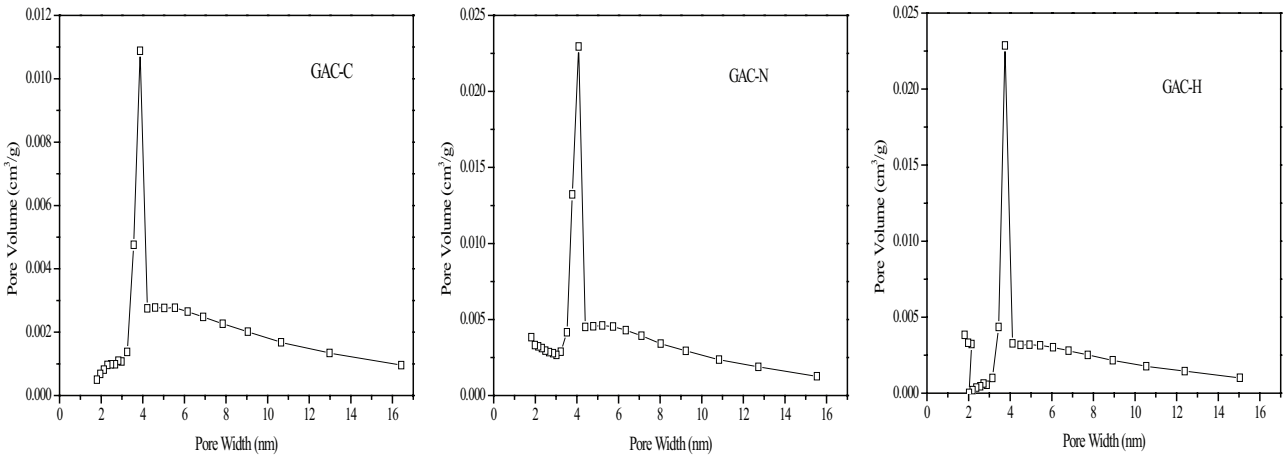

Fig. 2. Pore size distribution of GAC-C, GAC-N, and GAC-H.

Table 1
The porous structure parameters of GAC-C, GAC-N, and GAC-H

Sample	S_{BET} (m²/g)	S_{Micro} (m²/g)	S_{Meso} (m²/g)	V_{Micro} (cm³/g)	V_{Meso} (cm³/g)
GAC-C	16.51	0.9193	16.67	0.0004	0.0228
GAC-N	37.92	8.916	33.11	0.0045	0.0383
GAC-H	18.15	1.007	18.40	0.0004	0.0251

3.1.2. Surface morphology

SEM micrographs of the three samples are shown in Fig. 3. Compared with GAC-C, the surfaces of GAC-N and GAC-H were rougher, indicating the surface of raw adsorbent was corroded with nitric acid and hydrogen peroxide, and presented a rich mesoporous structure.

3.1.3. FTIR spectroscopy

The FTIR spectra of GAC-C, GAC-N, and GAC-H before and after MB adsorption are demonstrated in Fig. 4. Before MB adsorption, the major differences of the three samples were in the ranges of 1,000–1,200 cm^{-1} and 400–800 cm^{-1}. The bands around 3,430, 1,635, 1,385, and 1,035 cm^{-1} of all samples could be corresponding to O–H stretching of carboxyl group, C=O stretching of carboxylic acid [12] or N–H bending [31], the structure of the C–N bonds [32] or nitrate groups [24], and C=O stretch in cellulose and hemi-cellulose [1], respectively. Besides, the band at 1,120 cm^{-1} of GAC-N is attributed to C–O stretching in alcohol [30]. The bands between 400 and 800 cm^{-1} might be related to bending vibration of –OH, or stretching vibration of C–O groups [33]. After MB adsorption,

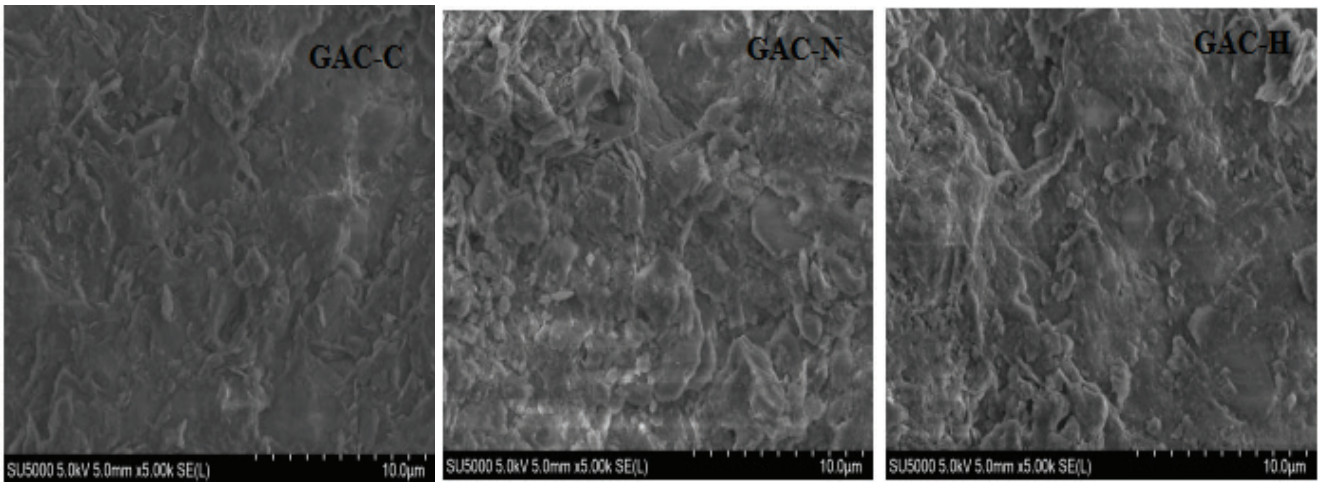

Fig. 3. SEM micrographs of GAC-C, GAC-N, and GAC-H.

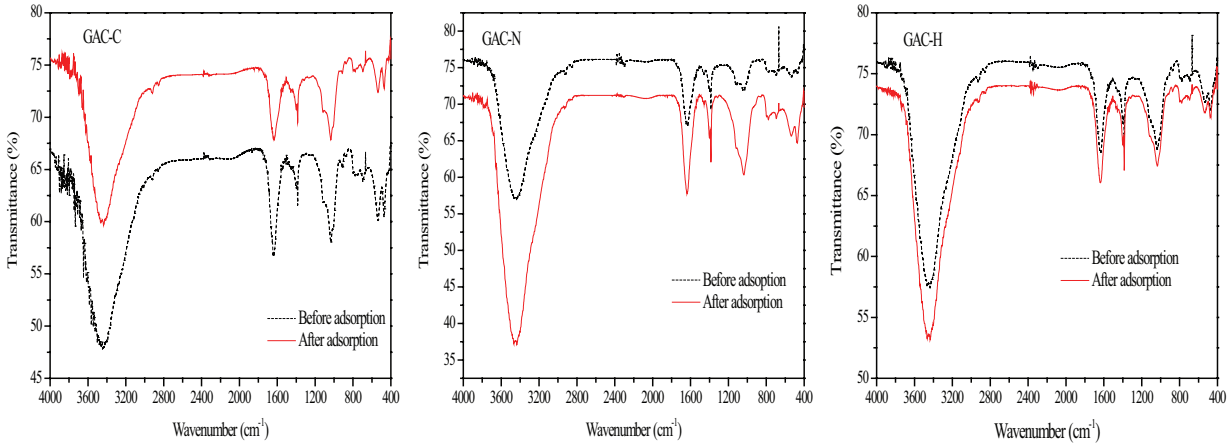

Fig. 4. FTIR spectrum of GAC-C, GAC-N, and GAC-H before and after adsorption.

the key bands of the three samples have a slight shift, while the peak intensity has also produced a certain change. These indicate that the above functional groups play an important role for the adsorption of MB.

3.2. Effect of operational parameters on MB adsorption

For chemical modification, modification temperature, modifier concentration, contact time [34], and adsorbent dose could generally affect the pore structure and surface chemistry properties of the activated carbon, which will significantly affect the MB adsorption capacity of modified activated carbon. Therefore, the effect of the above four factors on MB adsorption capacity is discussed in this section.

3.2.1. Effect of modification temperature on MB adsorption

When the modifier concentration, contact time, and adsorbent dose were 2 mol/L, 2 h, and 0.1 g/mL, respectively, the effect of modification temperature on MB adsorption was discussed and the results are presented in Fig. 5.

As shown in Fig. 5, with the increase of the modification temperature, the MB adsorption capacities of samples tend to increase. The reason may be that the increase of temperature accelerates the movement of the modifier molecules, and provides more heat for the reaction, causing that promotes the effect of modification agents on the activated carbon, and forms more functional groups [24] or mesopores which favor the adsorption of MB [32]. Besides, the MB adsorption capacities of samples modified by nitric acid are all greater. This may be due to the higher oxidation of nitric acid.

3.2.2. Effect of modifier concentration on MB adsorption

Fig. 6 shows the tendency of MB adsorption with the increase of modifier concentration. It can be seen that the MB adsorption of samples modified by nitric acid was declined with the increase of nitric acid concentration, while the MB adsorption of samples modified by hydrogen peroxide are first increased and then decreased. For nitric acid modification, with the increase of concentration, nitric acid oxidation is more and more intense, and will destroy the internal

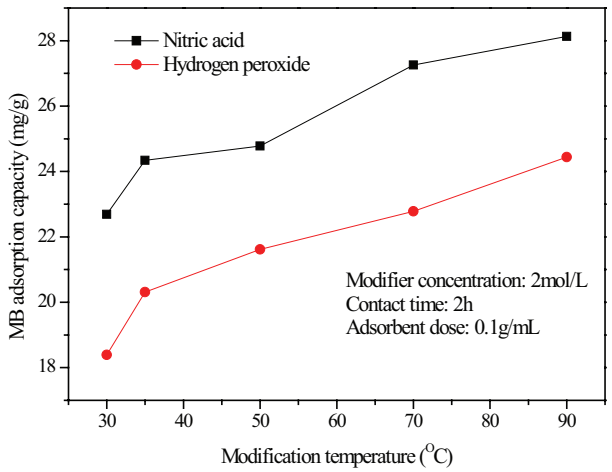

Fig. 5. Effect of modification temperature on MB adsorption.

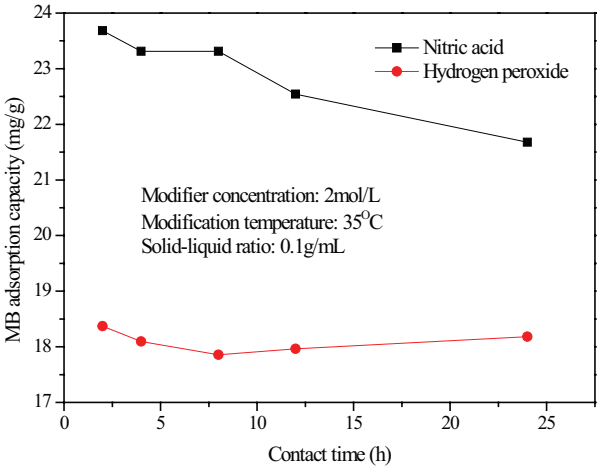

Fig. 7. Effect of contact time on MB adsorption.

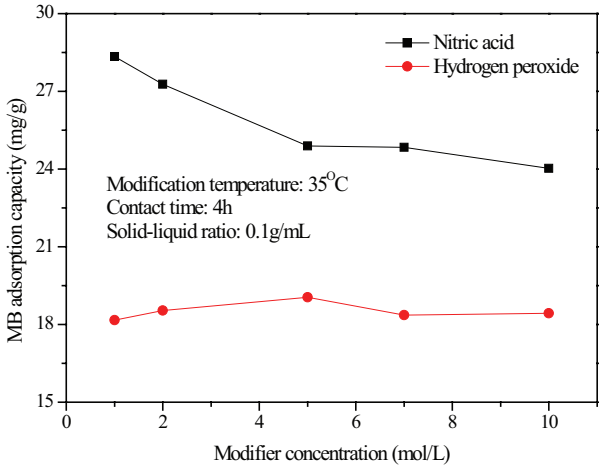

Fig. 6. Effect of modifier concentration on MB adsorption.

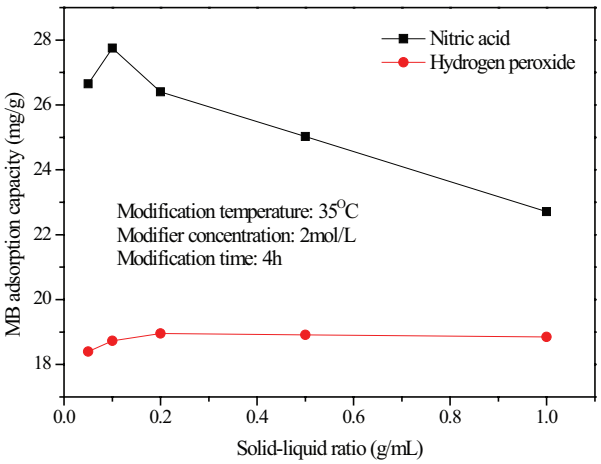

Fig. 8. Effect of adsorbent dose on MB adsorption.

structure of activated carbon, which makes the micropores and mesopores convert to macropores [22], leading to the reduce of MB adsorption of samples. Due to the relatively weak oxidizing power, much more mesopores are formed with modifier amount increase when the hydrogen peroxide concentrations are not more than 5 mol/L. However, with further increase of the hydrogen peroxide concentration, the mesopores are expanded into macropores, resulting in the reduction of MB adsorption.

3.2.3. Effect of contact time on MB adsorption

Theoretically, the long contact time is favorable for the oxidation reaction, resulting in the activated carbon forms more mesopores that improve the MB adsorption of samples, which has been confirmed by Qiu et al. [35]. On the contrary, the MB adsorption of all samples is generally decreasing with the extension of the contact time (Fig. 7). This might be due to the nature of the raw material itself and macroporous volume increase.

3.2.4. Effect of adsorbent dose on MB adsorption

Adsorbent dose is another important operational parameter for chemical modification of activated carbon. Unfortunately, there are few reports on this topic. Fig. 8 shows the variation of MB adsorption with the increase of adsorbent dose.

It is obvious that the modifiers are excessive when the adsorbent dose is lower, resulting in a large number of maropores in the sample. And with the continuous increase of adsorbent dose, the modifiers are penurious causing the oxidation reaction is incomplete which reduces the yield of mesopores.

3.3. Orthogonal tests and significance analysis of factors

In order to optimize modification conditions, the orthogonal methodology is often used in experiment [36]. Based on the discussion of operational conditions and other researches [22,24], an L9(3, 4) orthogonal array with four operational parameters (modified temperature (T_p), modifier

concentration (C), contact time (T), and adsorbent dose ($R_{S\text{-}L}$)) were designed. The details and the experimental results are listed in Table 2. The experimental results were the mean of the three experiments.

From Table 2, no. 7 experiment was the optimal process for both nitric acid and hydrogen peroxide modifications. Under the optimal conditions, MB adsorption capacities are 27.76 mg/g (HNO_3) and 26.77 mg/g (H_2O_2), respectively.

Table 3 shows the range analysis of the orthogonal experimental results. It is positive that the influence degree sequences of the four parameters for nitric acid and hydrogen peroxide modifications are very different. For the two modification processes, the most influential factors are modifier concentration (HNO_3) and modification temperature (H_2O_2), respectively. The significance analysis of factors at the significance level α = 0.10 (Table 4) also verifies this view.

Table 2
Orthogonal experimental details and results

No.	Factors				MB adsorption (mg/g)	
	T_p	C	T	$R_{S\text{-}L}$	HNO_3	H_2O_2
1	30	1	2	0.1	23.38	18.76
2	30	5	4	0.15	23.11	21.54
3	30	9	6	0.2	20.76	20.95
4	60	1	6	0.15	25.44	22.86
5	60	5	2	0.2	25.21	21.72
6	60	9	4	0.1	20.11	23.12
7	90	1	4	0.2	27.76	26.77
8	90	5	6	0.1	24.48	23.51
9	90	9	2	0.15	22.78	25.09

3.4. Optimum process

According to the analysis of operational parameters and orthogonal tests, the optimum process conditions for nitric acid and hydrogen peroxide modifications in this study are identical, and suggested as follows: modification temperature T_p = 90°C, modifier concentration C = 2 mol/L, contact time T = 4 h, and adsorbent dose $R_{S\text{-}L}$ = 0.2 g/mL. Figs. 9 and 10 show the adsorption isotherms and MB adsorption capacities at different times of the GAC-C, and samples modified under optimum process (GAC-N and GAC-H).

As shown in Figs. 9 and 10, the MB adsorption capacities of GAC-N and GAC-H are greater than GAC-C, indicating that the modification is beneficial to improve the MB adsorption of commercial GAC-C. The maximum MB adsorption

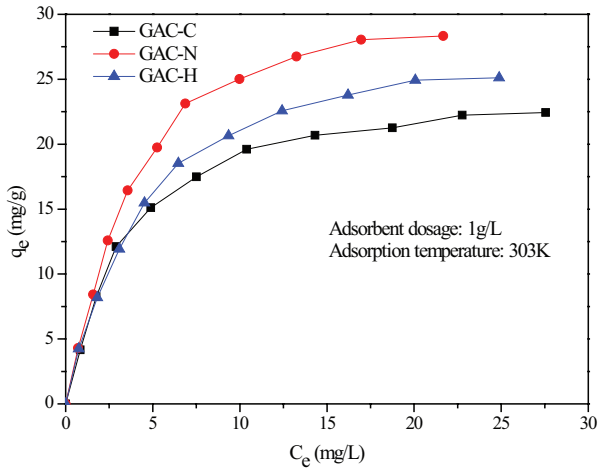

Fig. 9. The adsorption isotherms of GAC-C, GAC-N and GAC-H at 303 K.

Table 3
Range analysis of the orthogonal experimental results

Average	HNO_3 modification				H_2O_2 modification			
	T_p	C	T	$R_{S\text{-}L}$	T_p	C	T	$R_{S\text{-}L}$
X1	22.428	25.525	22.656	23.789	20.415	22.796	21.799	21.856
X2	23.587	24.398	23.776	23.659	22.565	22.255	23.161	23.809
X3	25.004	21.227	24.587	23.571	25.124	23.053	23.144	22.438
Range	2.576	4.298	1.931	0.218	4.709	0.798	1.362	1.953

Table 4
Significance analysis of factors for MB adsorption (α = 0.10)

Factors	Square of deviance		Freedom	F ratio		F critical values	Significance	
	HNO_3	H_2O_2		HNO_3	H_2O_2		HNO_3	H_2O_2
T_p	9.987	33.351	2	2.078	9.354	3.110		Yes
C	29.302	0.996	2	5.599	0.279	3.110	Yes	
T	5.643	3.665	2	0.917	1.028	3.110		
$R_{S\text{-}L}$	0.072	6.035	2	0.005	1.693	3.110		
Deviation	45.00	44.05	8					

capacities of GAC-C, GAC-N, and GAC-H are 22.44, 28.28, and 25.12 mg/g, respectively.

3.5. Adsorption isotherms and kinetics

3.5.1. Adsorption isotherms

The study of isotherms is very important for adsorption because it indicates the interaction of the adsorbates and adsorbents [28]. In this section, the Langmuir, Freundlich, and Temkin isotherm models [37,38] were used to analyze the adsorption data. Langmuir isotherm is a theoretical model, which assumes a monolayer adsorption without interactions between the adsorbent surface and adsorbate molecules. Freundlich isotherm is an empirical model, supposing the heterogeneous adsorption energies on the adsorbent surface are in existence. Temkin isotherm is especially used to describe the chemical adsorption process, and considers the heat of adsorption in layer linear reduces. The linear expressions of the three isotherms are as follows:

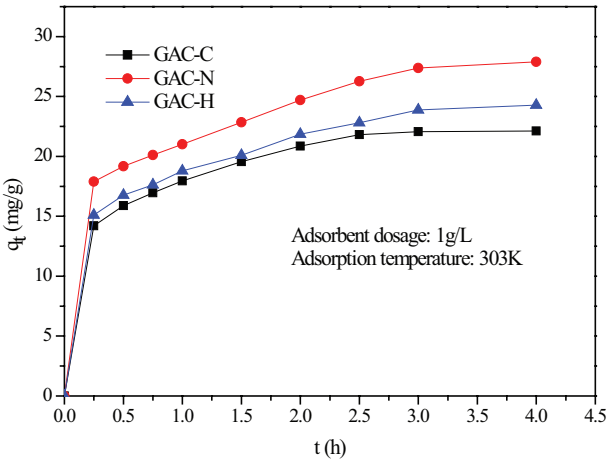

Fig. 10. MB adsorption capacities at time t of GAC-C, GAC-N, and GAC-H.

Langmuir isotherm

$$\frac{C_e}{q_e} = \frac{1}{q_{\max} K_L} + \frac{C_e}{q_{\max}} \tag{4}$$

Freundlich isotherm

$$\ln q_e = \ln K_F + \frac{1}{n} \ln C_e \tag{5}$$

Temkin isotherm

$$q_e = \frac{RT}{b_T} \ln K_T + \frac{RT}{b_T} \ln C_e \tag{6}$$

where $q_{\max}$ (mg/g) is the maximum adsorption capacity of the adsorbent, K_L (L/mg) is the Langmuir constant related to the adsorption capacity and adsorption rate; K_F ((mg/g)(mg/L)$^{1/n}$) and n are the Freundlich constants related to adsorption capacity and intensity, respectively; b_T (J/mol) is the Temkin constant related to the heat of adsorption, K_T (L/mg) is the Temkin isotherm constant, T (K) is the absolute temperature, and R is the universal gas constant.

The fitting results and constants of the three isotherm equations are shown in Fig. 11 and Table 5, respectively. It is evident that all R^2 values of Langmuir isotherm and Temkin isotherm are greater than 0.98, indicating the MB adsorption on to GAC-C, GAC-N, and GAC-H is a monolayer and chemical adsorption process. The n values of Freundlich isotherm are all in the range of 1–10, suggesting the MB adsorption is preferential. In addition, the maximum values of separation factor based on Langmuir isotherm ($R_L = 1/(1 + K_L C_{0,\max})$, $C_{0,\max}$ is the maximum initial MB concentration) [39] are 0.0666, 0.0794, and 0.0818, respectively, also certificating the MB adsorption is favorable. Furthermore, the maximum MB adsorption capacities from Langmuir isotherm are 25.57, 34.93, and 30.16 mg/g, respectively, which are more than the experimental results ($q_{\max,\exp}$).

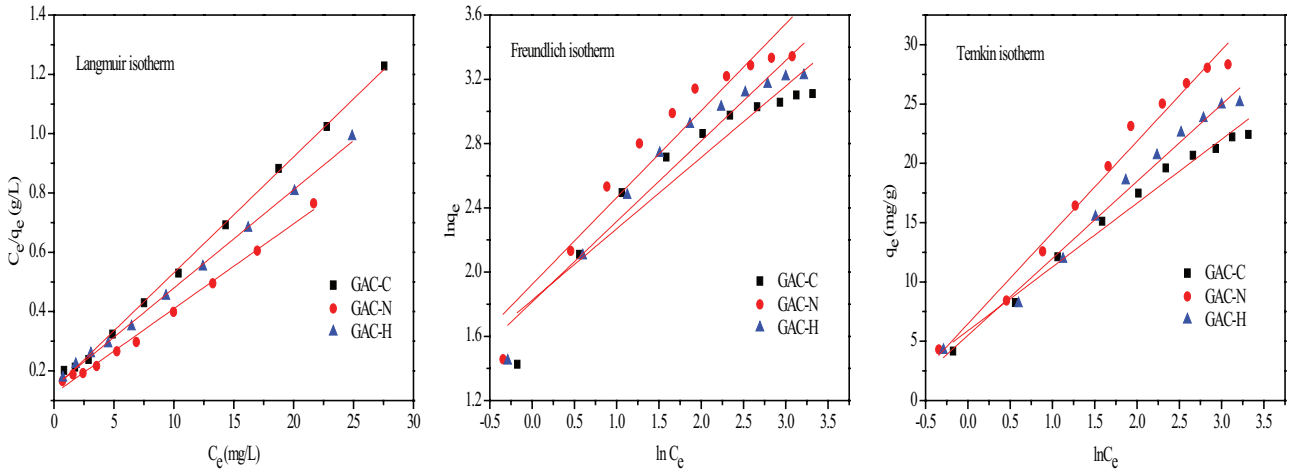

Fig. 11. Adsorption isotherms for MB adsorption on GAC-C, GAC-N, and GAC-H.

Table 5
Langmuir, Freundlich, and Temkin isotherm parameters for MB adsorption

Sample	$q_{max,exp}$	Langmuir isotherm			Freundlich isotherm			Temkin isotherm		
		q_{max}	K_L	R^2	K_F	n	R^2	b_T	K_T	R^2
GAC-C	22.44	25.57	0.2804	0.9984	60.75	2.250	0.8893	468.4	2.986	0.9812
GAC-N	28.33	34.93	0.2320	0.9936	35.01	1.849	0.9120	327.3	2.316	0.9812
GAC-H	25.12	30.16	0.2246	0.9983	37.34	1.996	0.9336	388.3	2.333	0.9862

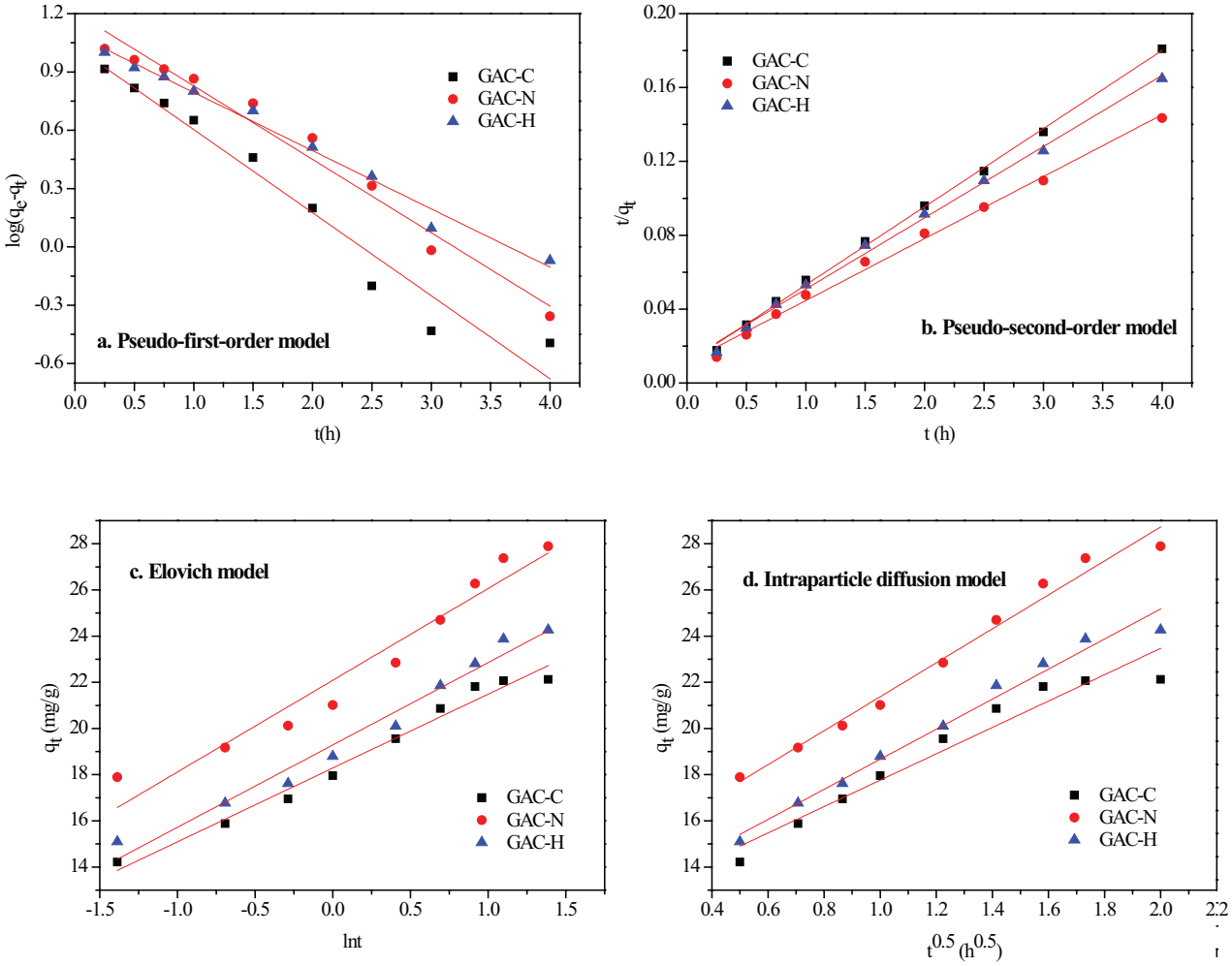

Fig. 12. Kinetics plots of MB adsorption on GAC-C, GAC-N, and GAC-H.

3.5.2. Adsorption kinetics

The pseudo-first-order, pseudo-second-order [40], Elovich, and intraparticle diffusion models [41] were employed to investigate the MB adsorption process in this section. The mathematical expressions of the four models are presented as follows:

Pseudo-first-order model

$$\log(q_e - q_t) = \log q_e - k_1 t \tag{7}$$

Pseudo-second-order model

$$\frac{t}{q_t} = \frac{1}{k_2 q_e^2} + \frac{t}{q_e} \tag{8}$$

Elovich model

$$q_t = \frac{1}{\beta}\ln(\alpha\beta) + \frac{1}{\beta}\ln t \tag{9}$$

Table 6
Kinetics parameters of different models for MB adsorption

Sample	$q_{e,exp}$ (mg/g)	Pseudo-first-order model			Pseudo-second-order model		
		$q_{e1,cal}$ (mg/g)	k_1 (1/h)	R^2	$q_{e2,cal}$ (mg/g)	k_2 (g/(mg·h))	R^2
GAC-C	22.44	10.73	0.4272	0.9520	23.62	0.1665	0.9981
GAC-N	28.33	16.05	0.3776	0.9702	29.81	0.1016	0.9939
GAC-H	25.12	12.38	0.2994	0.9846	25.91	0.1216	0.9956
Sample	$q_{t=1,exp}$ (mg/g)	Elovich model			Intraparticle diffusion model		
		α (mg/(g h))	β (g/mg)	R^2	k_i (mg/(g·h$^{0.5}$))	C	R^2
GAC-C	17.96	974.3	0.3127	0.9775	5.711	12.05	0.9377
GAC-N	21.01	1,031.2	0.2517	0.9422	7.354	14.02	0.9810
GAC-H	18.79	796.4	0.2804	0.9714	6.509	12.16	0.9796

Intraparticle diffusion model

$$q_t = k_i t^{0.5} + C \tag{10}$$

where k_1(1/h) is the pseudo-first-order rate constant, k_2 (g/(mg·h)) is the relevant adsorption rate constant of pseudo-second-order, α (mg/(g·h)) is the initial adsorption rate, β (g/mg) is the extent of surface coverage and activation energy for chemical adsorption, k_i (mg/(g·h$^{0.5}$)) is the constant of intraparticle diffusion rate, and C is the intercept, representing the thickness effects of the boundary layer.

Fig. 12 shows the fitting results of experimental MB adsorption data presented in Fig. 10 by different models. The kinetics parameters are listed in Table 6.

Comparing pseudo-first-order model and pseudo-second-order model, the fitting results of pseudo-second-order model are better, because of the higher R^2 values and the smaller errors between $q_{e,exp}$ and $q_{e2,cal}$ of which percentages are 5.27% (GAC-C), 5.21% (GAC-N), and 3.16% (GAC-H), respectively. Although the R^2 values of pseudo-first-order model are all greater than 0.95, the difference percentages of $q_{e,exp}$ and $q_{e1,cal}$ for the GAC-C, GAC-N, and GAC-H are 52.18%, 43.35%, and 50.72%, respectively, which are far beyond the error scope of statistical recognition.

α and β in Table 6, the MB adsorption capacities onto GAC-C, GAC-N, and GAC-H at 1 h calculated by Eq. (8) are 18.29, 22.09, and 19.29 mg/g, which are consistent with the experimental values ($q_{t=1,exp}$). Moreover, the values of 1/β which suggest the available number of adsorption sites for GAC-C, GAC-N, and GAC-H are 3.198, 3.974, and 3.566 mg/g, respectively, indirectly demonstrating that the MB adsorption capacities of GAC-N and GAC-H are higher than that of GAC-C.

As shown in Fig. 12 and Table 6, the fitting results of intraparticle diffusion model are also acceptable, declaring the intraparticle diffusion is the potential rate-controlling step of the MB adsorption processes. However, since the C values are not equal to zero, the fitting lines are through the origin. This is to say that there are thickness effects of the boundary layer in MB adsorption process.

4. Conclusions

In this study, a commercial GAC-C was used as raw adsorbent, and modified by nitric acid and hydrogen peroxide. With the analysis of operational parameters and orthogonal tests, the optimum modification conditions for nitric acid and hydrogen peroxide were the same and presented as follows: modification temperature T_p = 90°C, modifier concentration C = 2 mol/L, contact time T = 4 h, adsorbent dose $R_{S\text{-}L}$ = 0.2 g/mL. The MB adsorption capacities of GAC-C, GAC-N, and GAC-H are 22.44, 28.28 and 25.12 mg/g, respectively. The porous structure characterization showed that the mesopore volumes of GAC-N and GAC-H are greater than GAC-C. The FTIR analysis confirmed that the oxygen-containing functional groups played an important role in MB adsorption process. Moreover, the MB adsorption mechanism of GAC-C, GAC-N, and GAC-H was also discussed by using numerous adsorption models. The results indicated that MB adsorption was a heterogeneous and monolayer process in which chemisorption was dominant. The MB adsorption process could be well described by the pseudo-second-order model, and the intraparticle diffusion was the potential rate-controlling step, while there were the thickness effects of the boundary layer in MB adsorption process.

Acknowledgments

This work was supported by Project supported by the State Key Program of National Natural Science of China (51638006), Guangxi young and middle-aged teachers basic ability promotion project (2017KY0244), Guangxi Scientific Experiment Center of Mining, Metallurgy and Environment (KH2012ZD004), the project of high level innovation team and outstanding scholar in Guangxi colleges and universities (002401013001), Guangxi science and technology program (Guike AD17195023), and Special Funding for Guangxi 'BaGui Scholar' Construction Projects.

References

[1] F. Kallel, F. Chaari, F. Bouaziz, F. Bettaieb, R. Ghorbel, S.E. Chaabouni, Sorption and desorption characteristics for the removal of a toxic dye, methylene blue from aqueous solution by a low cost agricultural by-product, J. Mol. Liq., 219 (2016) 279–288.
[2] A. Sandoval, C. Hernández-Ventura, T.E. Klimova, Titanate nanotubes for removal of methylene blue dye by combined adsorption and photocatalysis, Fuel, 198 (2017) 22–30.
[3] T.H. Liu, Y.H. Li, Q.J. Du, J.K. Sun, Y.Q. Jiao, G.M. Yang, Z.H. Wang, Y.Z. Xia, W. Zhang, K.L. Wang, H.W. Zhu, D.H. Wu, Adsorption of methylene blue from aqueous solution by graphene, Colloids Surf., B, 90 (2012) 197–203.

[4] J.M. Duan, R.C. Liu, T. Chen, B. Zhang, J.D. Liu, Halloysite nanotube-Fe_3O_4 composite for removal of methyl violet from aqueous solutions, Desalination, 293 (2012) 46–52.
[5] A.K. Hammed, N. Dewayanto, D. Du, M.H.A. Rahim, M.R. Nordin, Novel modified ZSM-5 as an efficient adsorbent for methylene blue removal, J. Environ. Chem. Eng., 4 (2016) 2607–2616.
[6] W.W. Yuan, P. Yuan, D. Liu, W.B. Yu, M.W. Laipan, L.L. Deng, F.R. Chen, In situ hydrothermal synthesis of a novel hierarchically porous TS-1/modified-diatomite composite for methylene blue (MB) removal by the synergistic effect of adsorption and photo-catalysis, J. Colloid Interface Sci., 462 (2016) 191–199.
[7] U. Pal, A. Sandoval, S.I.U. Madrid, G. Corro, V. Sharma, P. Mohanty, Mixed titanium, silicon, and aluminum oxide nanostructures as novel adsorbent for removal of rhodamine 6G and methylene blue as cationic dyes from aqueous solution, Chemosphere, 163 (2016) 142–152.
[8] Y.H. Li, Q.J. Du, T.H. Liu, X.J. Peng, J.J. Wang, J.K. Sun, Y.H. Wang, S.L. Wu, Z.H. Wang, Y.Z. Xia, L.H. Xia, Comparative study of Methylene Blue dye adsorption onto activated carbon, graphene oxide, and carbon nanotubes, Chem. Eng. Res. Des., 91 (2013) 361–368.
[9] B.H. Hameed, A.T. Din, A.L. Ahmad, Adsorption of methylene blue onto bamboo-based activated carbon: kinetics and equilibrium studies, J. Hazard. Mater., 141 (2007) 819–825.
[10] M. Dogan, M. Alkan, Ö. Demirbas, Y. Özdemir, C. Özmetin, Adsorption kinetics of maxilon blue GRL onto sepiolite from aqueous solutions, Chem. Eng. J., 124 (2006) 89–101.
[11] D.Z. Shen, J.X. Fan, W.Z. Zhou, B.Y. Gao, Q.Y. Yue, Q. Kang, Adsorption kinetics and isotherm of anionic dyes onto organo-bentonite from single and multi-solute systems, J. Hazard. Mater., 172 (2009) 99–107.
[12] S. Shakoor, A. Nasar, Removal of methylene blue dye from artificially contaminated water using citrus limetta peel waste as a very low cost adsorbent, J. Taiwan Inst. Chem. Eng., 66 (2016) 154–163.
[13] A. Bhatnagar, M. Sillanpää, Utilization of agro-industrial and municipal waste materials as potential adsorbents for water treatment—a review, Chem. Eng. J., 157 (2010) 277–296.
[14] A. Mittal, J. Mittal, A. Malviya, D. Kaur, V.K. Gupta, Adsorption of hazardous dye crystal violet from wastewater by waste materials, J. Colloid Interface Sci., 343 (2010) 463–473.
[15] Q. Li, Y.H. Li, X.M. Ma, Q.J. Du, K.Y. Sui, D.C. Wang, C.P. Wang, H.L. Li, Y.Z. Xia, Filtration and adsorption properties of porous calcium alginate membrane for methylene blue removal from water, Chem. Eng. J., 316 (2017) 623–630.
[16] R.S.P. Teixeira, R.J. Correa, J.S. Bello Forero, M.G.S. Silva, R.C.S. Oliveir, R.S. Souza, Comparative study of PEO and PVA hydrogels for removal of methylene blue dye from wastewater, J. Appl. Polym. Sci., 134 (2017). doi: 10.1002/APP.45043.
[17] M.A. Islam, M.J. Ahmed, W.A. Khanday, M. Asif, B.H. Hameed, Mesoporous activated carbon prepared from NaOH activation of rattan (*Lacosperma secundiflorum*) hydrochar for methylene blue removal, Ecotoxicol. Environ. Saf., 138 (2017) 279–285.
[18] D. Dutta, D. Thakur, D. Bahadur, SnO_2 quantum dots decorated silica nanoparticles for fast removal of cationic dye (methylene blue) from wastewater, Chem. Eng. J., 281 (2015) 482–490.
[19] B. Mudyawabikwa, H.H. Mungondori, L. Tichagwa, D.M. Katwire, Methylene blue removal using a low-cost activated carbon adsorbent from tobacco stems: kinetic and equilibrium studies, Water Sci. Technol., 75 (2017) 2390–2402.
[20] Z.X. Jiang, Y. Liu, X.P. Sun, F.P. Tian, F.X. Sun, C.H. Liang, W.S. You, C.R. Han, C. Li, Activated carbons chemically modified by concentrated H_2SO_4 for the adsorption of the pollutants from waste water and the dibenzothiophene from fuel oils, Langmuir, 19 (2003) 731–736.
[21] S.B. Wang, Z.H. Zhu, A. Coomes, F. Haghseresht, G.Q. Lu, The physical and surface chemical characteristics of activated carbons and the adsorption of methylene blue from wastewater, J. Colloid Interface Sci., 284 (2005) 440–446.
[22] F. Güzel, H. Sayğılı, G.A. Sayğılı, F. Koyuncu, C. Yılmaz, Optimal oxidation with nitric acid of bio-char derived from pyrolysis of weeds and its application in removal of hazardous dye methylene blue from aqueous solution, J. Cleaner Prod., 144 (2017) 260–265.
[23] F. Hatami, H. Faghihian, Modification of activated carbon by 4-(8-hydroxyquinoline-azo) benzamidine for removal of Hg^{2+} from aqueous solutions, Environ. Prog. Sustainable Energy, 34 (2015) 1562–1567.
[24] Y. Gokce, Z. Aktas, Nitric acid modification of activated carbon produced from waste tea and adsorption of methylene blue and phenol, Appl. Surf. Sci., 313 (2014) 352–359.
[25] H. ShamsiJazeyi, T. Kaghazchi, Investigation of nitric acid treatment of activated carbon for enhanced aqueous mercury removal, J. Ind. Eng. Chem., 16 (2010) 852–858.
[26] K. Sun, J.C. Jiang, D.D. Cui, Preparation of activated carbon with highly developed mesoporous structure from *Camellia oleifera* shell through water vapor gasification and phosphoric acid modification, Biomass Bioenergy, 35 (2011) 3643–3647.
[27] M.-C. Shih, Kinetics of the batch adsorption of methylene blue from aqueous solutions onto rice husk: effect of acid-modified process and dye concentration, Desal. Wat. Treat., 37 (2012) 200–214.
[28] L. Zhou, J.C. Huang, B.Z. He, F.A. Zhang, H.B. Li, Peach gum for efficient removal of methylene blue and methyl violet dyes from aqueous solution, Carbohydr. Polym., 101 (2014) 574–581.
[29] L. Zhou, B.Z. He, J.C. Huang, One-step synthesis of robust amine- and vinyl-capped magnetic iron oxide nanoparticles for polymer grafting, dye adsorption, and catalysis, ACS Appl. Mater. Interfaces, 5 (2013) 8678–8685.
[30] L.H. Liu, Y. Lin, Y.Y. Liu, H. Zhu, Q. He, Removal of methylene blue from aqueous solutions by sewage sludge based granular activated carbon: adsorption equilibrium, kinetics, and thermodynamics, J. Chem. Eng. Data, 58 (2013) 2248–2253.
[31] X. Tang, C. Dai, C. Li, W.H. Liu, S.T. Gao, C. Wang, Removal of methylene blue from aqueous solution using agricultural residue walnut shell: equilibrium, kinetic, and thermodynamic studies, J. Chem., (2017) 1–10.
[32] X.Y. Ge, X.F. Ma, Z.S. Wu, X.M. Xiao, Y.J. Yan, Modification of coal-based activated carbon with nitric acid using microwave radiation for adsorption of phenanthrene and naphthalene, Res. Chem. Intermed., 41 (2015) 7327–7347.
[33] L.H. Liu, Y. Lin, Y.Y. Liu, Q. He, Effect of binders on porous properties, surface chemical properties and adsorption characteristics of granular adsorbents from sewage sludge, Mater. Sci., 20 (2014) 488–492.
[34] C.J. Chen, X. Li, Z.F. Tong, Y. Li, M.F. Li, Modification process optimization, characterization and adsorption property of granular fir-based activated carbon, Appl. Surf. Sci., 315 (2014) 203–211.
[35] J.H. Qiu, G.H. Wang, Y.C. Bao, D.L. Zeng, Y. Chen, Effect of oxidative modification of coal tar pitch-based mesoporous activated carbon on the adsorption of benzothiophene and dibenzothiophene, Fuel Process. Technol., 129 (2015) 85–90.
[36] H. Deng, G.L. Zhang, X.L. Xu, G.H. Tao, J.L. Dai, Optimization of preparation of activated carbon from cotton stalk by microwave assisted phosphoric acid-chemical activation, J. Hazard. Mater., 182 (2010) 217–224.
[37] M.G. Vaz, A.G.B. Pereira, A.R. Fajardo, A.C.N. Azevedo, F.H.A. Rodrigues, Methylene blue adsorption on chitosan-g-poly(acrylic acid)/rice husk ash super absorbent composite: kinetics, equilibrium, and thermodynamics, Water Air Soil Pollut., 228 (2017) 14.
[38] Z.H. Cheng, J. Liao, B.Z. He, F. Zhang, F.A. Zhang, X.H. Huang, L. Zhou, One-step fabrication of graphene oxide enhanced magnetic composite gel for highly efficient dye adsorption and catalysis, ACS Sustainable Chem. Eng., 3 (2015) 1677–1685.
[39] M.J. Ahmed, S.K. Dhedan, Equilibrium isotherms and kinetics modeling of methylene blue adsorption on agricultural wastes-based activated carbons, Fluid Phase Equilib., 317 (2012) 9–14.
[40] G.S. Gong, F.A. Zhang, Z.H. Cheng, L. Zhou, Facile fabrication of magnetic carboxymethyl starch/poly(vinylalcohol) composite gel for methylene blue removal, Int. J. Biol. Macromol., 81 (2015) 205–211.
[41] L. Sun, D.M. Chen, S.G. Wan, Z.B. Yu, Performance, kinetics, and equilibrium of methylene blue adsorption on biochar derived from eucalyptus saw dust modified with citric, tartaric, and acetic acids, Bioresour. Technol., 198 (2015) 300–308.